Light trapping enhancement in thin film silicon solar cells with different front and back grating periodicities

Renchen Liu (刘仁臣), Zihuan Xia (夏子奂), Yonggang Wu (吴永刚)*, Hongfei Jiao (焦宏飞), Zhaoming Liang (梁钊铭), and Jian Zhou (周 建)

Institute of Precision Optical Engineering, Tongji University, Shanghai 200092, China

**Corresponding author: ygwu@tongji.edu.cn*

Received July 17, 2013; accepted November 5, 2013; posted online December 9, 2013

Dual-grating structure thin-film silicon solar cells with different front and back grating periodicities are designed The geometrical parameters of both gratings are investigated. The reflection is greatly reduced by the front grating, whereas the absorption in the long wavelength is increased because of the back grating. The short circuit current of the combined structure is enhanced by 16.8% for a 1-μm thick c-Si layer compared with that of the conformal grating structure. The short circuit current can be further increased by creating a relative lateral displacement between the front and back gratings. The displacement results in a more remarkably enhanced absorption when the thickness of the active layer is reduced, indicating its importance in the design of ultra-thin high-efficiency solar cells.

OCIS codes: 050.2770, 350.2770, 350.6050.
doi: 10.3788/COL201311.120501.

Grating structures are intentionally introduced into thin-film solar cells because they can be used either as front coupler to diffract the incident light into a waveguide or as advanced back reflectors to increase both the path length and the spectral density of optical modes at long wavelengths[1−4]. Conformal dual grating structures are commonly employed in thin-film solar cells, and substantial enhancement of the optical path and the electric field intensity in the active layer are observed when the guided modes are achieved, resulting in remarkable increase in absorption at the resonant wavelengths[5−8]. However, increasing light coupling into waveguide modes and optical path length in active layers requires judicious selection of structural parameters of the front and back gratings. In addition, the out-coupling effect resulting from the structure consisting of front and back symmetric gratings with an identical period will likely reduce the efficiency of a solar cell, similar to that observed for a symmetric single grating, which can be explained by the reciprocity theorem[1,9,10].

In this letter, misaligned dual grating structures with different front and back grating periodicities are proposed. The front and back grating structures are optimized separately to achieve an efficient anti-reflection front surface and an advanced back reflector, respectively. The two optimum structures are then combined, and the effects of the relative lateral displacement between the front and back gratings are investigated.

Wavelength-dependent refractive indices for the c-Si, transparent conducting ZnO, and Ag are obtained from Ref. [11]. The simulations are performed using the rigorous coupled-wave analysis (RCWA) of Rsoft DiffractMod[12]. In the simulation, unpolarized sunlight is assumed to strike normally at the top of the solar cells, unless mentioned otherwise. The short circuit current density $J_{\rm sc}$, which characterizes the overall efficiency of a solar cell, is adopted as the function for evaluation. $J_{\rm sc}$ enhancement is defined as $(J_{\rm sc}-J_{\rm scr})/J_{\rm scr}$, where $J_{\rm scr}$ is the short circuit current density of the reference structure. All generated electron-hole pairs are assumed to contribute to the photocurrent. $J_{\rm sc}$ over the wavelength range from 400 to 1100 nm is given by

$$J_{\rm sc}=e\int_{400\ \rm nm}^{1100\ \rm nm}\frac{\lambda}{hc}A(\lambda)I_{\rm AM1.5}(\lambda){\rm d}\lambda, \tag{1}$$

where e is the charge of an electron, λ is the wavelength, h is Planck's constant, c is the speed of light in free space, A is the absorption in the active volume, and $I_{\rm AM1.5}$ is the AM 1.5 solar spectrum[13]. The front, back, and combined structures are presented in Fig. 1.

The front grating structure of the solar cells is supposed to reduce the reflection of the solar cells. Spectrally averaged reflectance ${\rm RW}_i$ of the ith order reflectance over the wavelength range from 400 to 1100 nm, which characterizes the overall reflectance of a solar cell, is defined as

$${\rm RW}_i=\frac{\sum\limits_{\lambda}R_i(\lambda)I_{\rm AM1.5}(\lambda)}{N}, \tag{2}$$

where i is the diffraction order, R_i is the reflectance of the ith order (obtained by RCWA), and N is the total number of the calculated wavelengths.

Here, we consider a sinusoidal grating structure consisting of ZnO/c-Si with an 80-nm homogeneous ZnO layer on top as an anti-reflector. A semi-infinite c-Si medium is adopted as the substrate to eliminate the effect of the back structure on the calculation of the spectrally

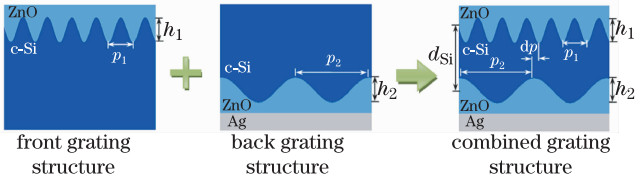

Fig. 1. Schematic of the proposed thin-film silicon solar cell. The combined grating structure is composed of the front and back grating structures.

averaged reflectance. The reflectance characteristic of the front grating structure is explored by scanning the period p_1 and height h_1 of the front grating, and the obtained total RW is shown in Fig. 2. Total RW gradually increases with increasing p_1, and further calculation of RW_i indicates that the contribution of high-order reflectance dominates the total spectrally averaged reflectance. This phenomenon can be attributed to the large period that supports the high-order diffraction modes outside the cell. When h_1 is increased to 300 nm, an excellent impedance matching between air and silicon is obtained. When $p_1 < 300$ nm and $h_1 > 200$ nm, the total RW is <2%, which indicates that efficient anti-reflection surface is obtained. However, considering the technologically feasible requirement on the geometrical parameters, $p_1$values >300 nm are preferred. Therefore, h_1=300 and p_1=300 nm are selected for the front grating structure.

The back grating structure is expected to diffract the incident light into a larger propagating angle, thereby increasing the optical path length and potentially trapping light into guided modes in the active layer. Therefore, the zero-order reflectance should be restrained, and a relatively large higher order reflectance is preferred. To achieve this goal, a sinusoidal grating is placed on an 80-nm ZnO barrier. The back reflection electrode is a 300-nm-thick Ag layer. The period p_2 and height h_2 of the back grating are optimized, as shown in Fig. 3.

Given the complexity of the calculated RW_0 and RW_1 as functions of p_2 and h_2, we choose the optimum height h_2 and period p_2 judiciously, such that a compromise is considered between the large h_2 and p_2 values to reduce the zero-order reflectance and the relatively small ones to increase high-order reflectance. A very low RW_0 with a relatively high RW_1 is observed when the p_2 and h_2 are 900 and 200 nm, respectively. This structure is therefore selected for the back grating structure.

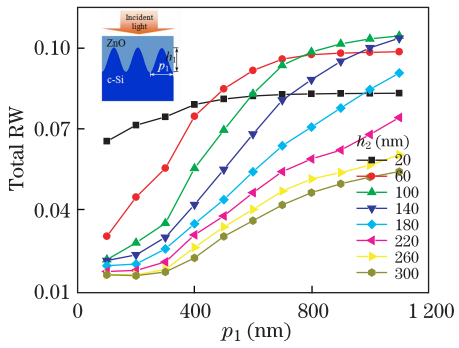

Fig. 2. Total RW as a function of p_1 at different values of h_1 of the front grating.

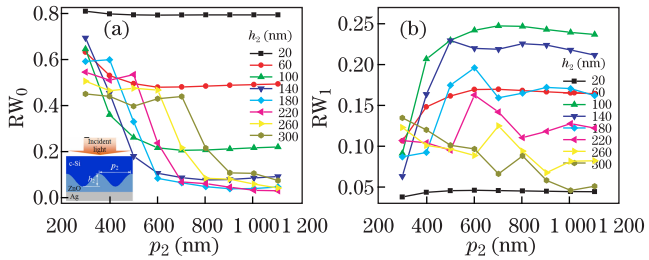

Fig. 3. (a) RW_0 and (b) RW_1 as functions of p_2 at different values of h_2 of the back grating.

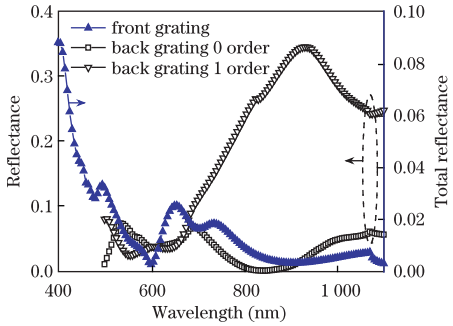

Fig. 4. (Color online) Total reflectance as a function of wavelength for the optimum front grating structure (blue triangle) and the zero-order (black square) and first-order reflectances (black triangle) as a function of wavelength for the optimum back grating structure.

The total reflectance of the optimum front grating structure, as well as the zero-order and first-order reflectances of the optimum back grating structure, is shown in Fig. 4. The total reflectance of the front grating structure is extremely low, and an average reflectance of 1.63% is obtained. For the back grating structure, the zero-order reflectance over the entire calculated wavelength is very low, while the first-order reflectance is relatively high, especially for long wavelengths.

The combined structure is illustrated in Fig. 1. The thicknesses of the uniform front and back ZnO layers and Ag back electrode layer are assumed to be 80, 80, and 300 nm, respectively. The periods of the front and back grating layers and the heights of the front and back grating layers are 300, 900, 300, and 200 nm, respectively. The relative lateral displacement between the front and back gratings and the thickness of the active layer are designated as dp and d_{si}, respectively. Given that the period of the back grating is thrice as large as that of the front grating, the dimension of the simulation window is selected as the period of the back grating. The number of the harmonics of the Fourier series is chosen to be 101, and the convergence criteria of all calculated reflectance and absorption are set to 10^{-6}.

Several studies have shown that the maximum short circuit current of the conformal grating structure ($p_1 = p_2 = 600$ nm, $h_1 = h_2 = 300$ nm) can be achieved[6,14,15]. For a 1-μm-thick c-Si solar cell, the absorptance spectra of the flat structure ($h_1 = h_2 = 0$), the conformal grating structure, and the combined grating structures with or without relative lateral displacement are calculated and shown in Fig. 5. Compared with the conformal grating structure, the combined grating structure of our design shows higher absorption in both short and long wavelength ranges. The enhanced absorption in the short wavelength is due to the effective anti-reflection effect of the front grating structure, whereas enhanced absorption in the long wavelength is attributed to the efficient coupling of light into the guided modes by the back grating structure.

The absorption can be further increased by introducing the relative lateral displacement between the front and back gratings (Fig. 5). The J_{sc} values of the conformal grating structure and the combined grating structure without and with relative lateral displacement are 16.02, 18.71, and 19.86 mA/cm^2, respectively. The correspond-

ing J_{sc} enhancements of the second structure to the first and the last to the second structure are 16.8% and 6.1%, respectively. The combined grating structure with a relative lateral displacement reaches a 45.8% J_{sc} enhancement compared with the value 13.62 mA/cm^2 J_{sc} of the flat structure.

For the active layer thickness d_{si} of 300, 500, and 1000 nm, the J_{sc} and J_{sc} enhancement of the grating structures are calculated and shown in Fig. 6. The highest J_{sc} enhancement of 11.1% is achieved by the misaligned structure with the 300-nm active layer, which shows a great potential advantage of the misalignment for the ultra-thin solar cells to achieve high efficiency. The higher J_{sc} enhancement of thinner d_{si} may be attributed to the stronger interactions of the front and back gratings.

The absorption as a function of the wavelength and the thickness of the active layer, d_{Si}, for the aligned grating structure (dp= 0) and the misaligned grating structure (dp = $\pi/4$) under TE incidence are shown in Fig. 7. The resonance modes in the aligned grating structure remain, and additional resonance modes appear in the misaligned grating structure. For visual clarity, white lines are added to indicate these additional resonance modes. These modes are derived from the split of the degenerate modes of the aligned grating structures, which can be attributed to the symmetrical disruption in the misaligned grating structures. An identical conclusion is derived for TM incidence.

We have also calculated the absorption of triangular and trapezoidal grating structures with and without relative lateral displacement under TE polarization incidence. The scattering property of the grating is changed, which results in the variation of absorption. However, relatively higher absorption and additional resonance modes can still be achieved by intentionally introducing the relative lateral displacement.

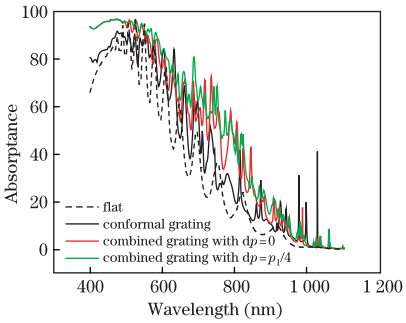

Fig. 5. (Color online) Absorption spectra of the flat structure, conformal grating structure, and combined grating structures with d_{si} = 1000 nm.

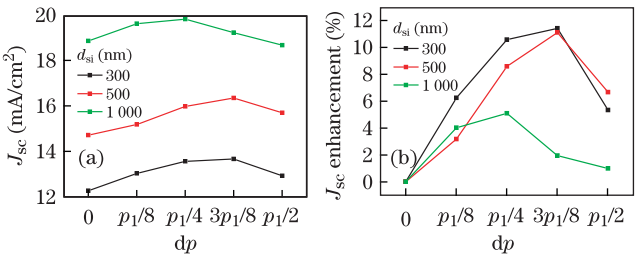

Fig. 6. (Color online) (a) J_{sc} and (b) J_{sc} enhancement as functions of dp with various d_{si} values.

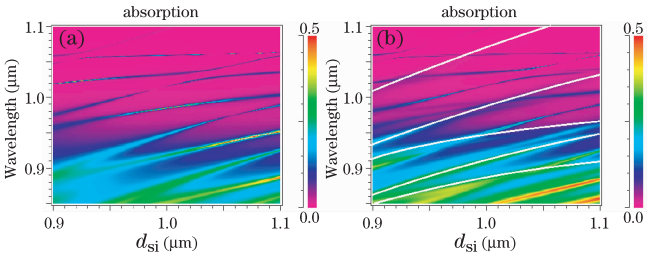

Fig. 7. Absorption spectra as functions of wavelengths and Si active layer thickness for (a) dp= 0 and (b) dp = p_1/4.

In conclusion, thin-film silicon solar cells with different front and back grating periodicities are designed and optimized. The period and height of both gratings are investigated separately to achieve an efficient anti-reflection structure at the front surface and a large-angle diffraction structure at the back surface. The spectral properties are analyzed, and the performance of the combined grating structure is simulated. Enhanced absorption of the combined structure over the entire calculated wavelength is observed and compared with that of the conformal grating. A 16.8% enhancement of J_{sc} is achieved for a 1-μm-thick c-Si layer. J_{sc} can be further increased by 6.1%, considering the relative lateral displacement between the front and back gratings. An 11.1% increase is obtained for the ultra-thin (300 nm) c-Si active layer, which indicates that the displacement is crucial in the design of ultra-thin high-efficiency solar cells.

This work was supported by the National Natural Science Foundation of China (No. 60977028) and the Key Project Foundation of Shanghai (No. 09JC1413800).

References

1. S. Mokkapati and K. R. Catchpole, J. Appl. Phys. **112,** 101101 (2012).
2. E. R. Martins, J. Li, Y. Liu, J. Zhou, and T. F. Krauss, Phys. Rev. B **86,** 041404 (2012).
3. A. Abass, H. H. Shen, P. Bienstman, and B. Maes, J. Appl. Phys. **109** (2011).
4. G. Li, H. Zhen, Z. Huang, K. Li, W. Shen, and X. Liu, Chin. Opt. Lett. **10,** 012401 (2012).
5. M. G. Deceglie, V. E. Ferry, A. P. Alivisatos, and H. A. Atwater, Nano Lett. **12,** 2894 (2012).
6. D. Madzharov, R. Dewan, and D. Knipp, Opt. Express **19,** A95 (2011).
7. J. Zhu, C.-M. Hsu, Z. Yu, S. Fan, and Y. Cui, Nano Lett. **10,** 1979 (2009).
8. Z. Xia, Y. Wu, R. Liu, Z. Liang, J. Zhou, and P. Tang, Opt. Express **21,** A548 (2013).
9. A. T. de Hoop, Appl. Sci. Res. B **8,** 135 (1960).
10. C. Heine and R. H. Morf, Appl. Opt. **34,** 2476 (1995).
11. "Refractive index database", retrieved 2012, http://refractiveindex.info.
12. Rsoft, "DiffractMod" (2010), retrieved 2010, www.rsoftdesign.com.
13. NREL, "Reference Solar Spectral Irradiance: Air Mass 1.5", retrieved 2012, http://rredc.nrel.gov/solar/spectra/am1.5/.
14. C. Haase and H. Stiebig, Prog. Photovolt. Res. Appl. **14,** 629 (2006).
15. R. Dewan and D. Knipp, J. Appl. Phys. **106,** 074901 (2009).